Radio Core Dominance of Fermi Blazars

Matt Zhiyuan Pei (裴致远)
Dottorando@
Dipartimento di Fisica e Astronomia, Università di Padova
& INFN

Co-with Prof. Denis Bastieri
& Prof. J-H Fan (樊军辉, Guangzhou University)

11/06/2018, Torino, IT

Outline

- 1. Introduction to Active Galactic Nuclei and Beaming Effect;
- 2. Fermi Large Area Telescope;
- 3. Core-Dominance Parameter and Data Analysis;
- 4. Correlation between Spectral Index and Core-Dominance Parameter;
- 5. Summary and Discussion.

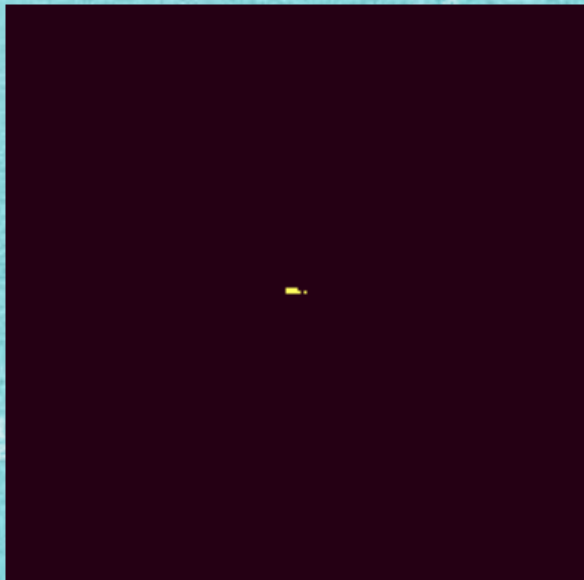

Outline

- 1. Introduction to Active Galactic Nuclei and Beaming Effect;
- 2. Fermi Large Area Telescope;
- 3. Core-Dominance Parameter and Data Analysis;
- 4. Correlation between Spectral Index and Core-Dominance Parameter;
- 5. Summary and Discussion.

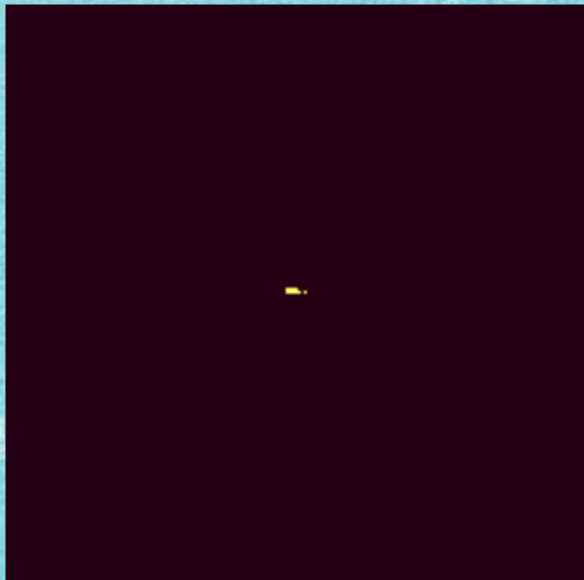

1.1 Standard model for Active Galactic Nuclei (AGNs)

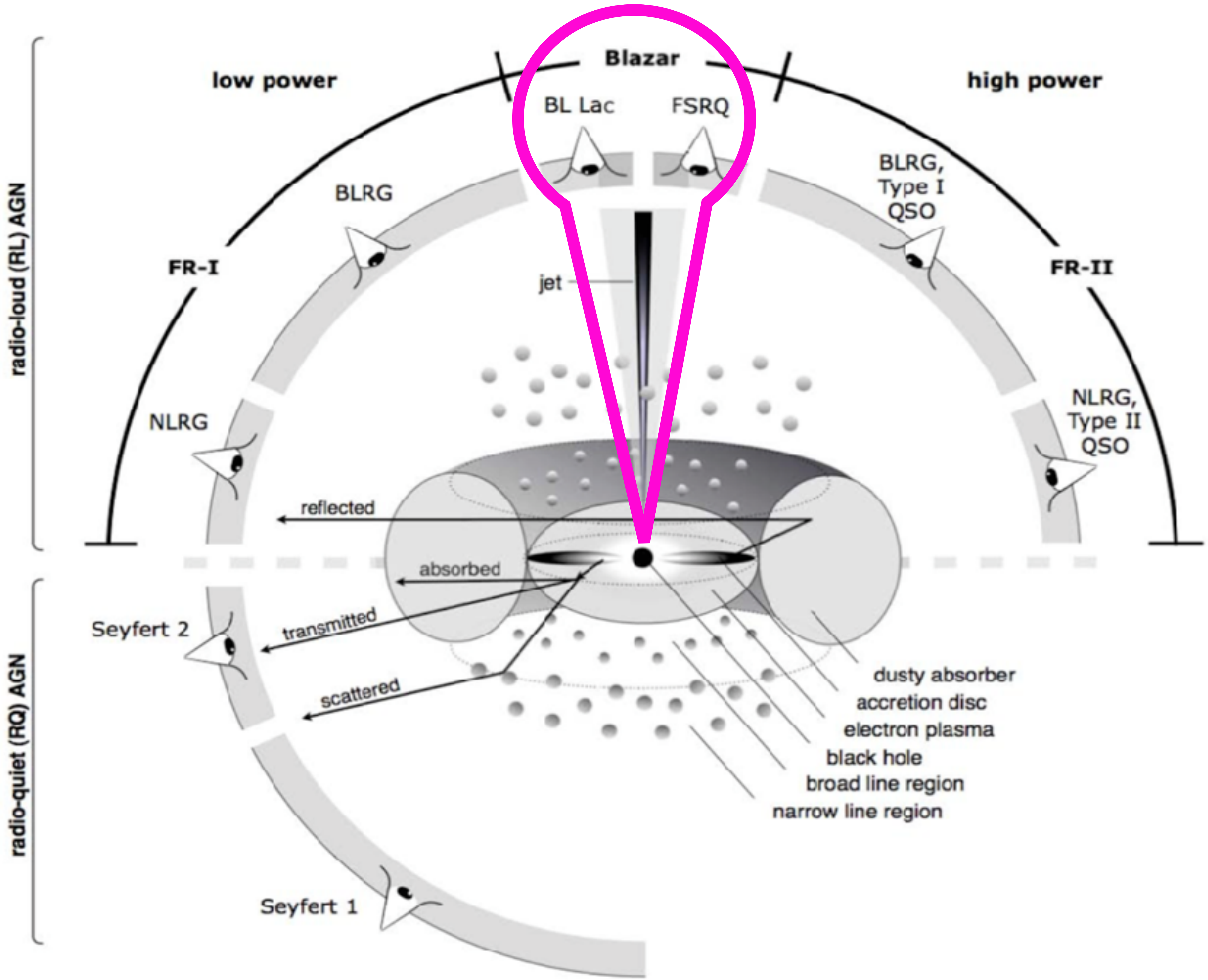

radio-loud (RL) AGN
radio-quiet (RQ) AGN
low power
Blazar
high power
BL Lac
FSRQ
BLRG
BLRG,
Type I
QSO
FR-I
FR-II
jet
NLRG
NLRG,
Type II
QSO
reflected
absorbed
transmitted
scattered
Seyfert 2
dusty absorber
accretion disc
electron plasma
black hole
broad line region
narrow line region
Seyfert 1

Blazar spectra

- Blazar spectra are characterised by two bumps, well fitted by synchrotron and inverse-Compton emission of high-energy electrons.

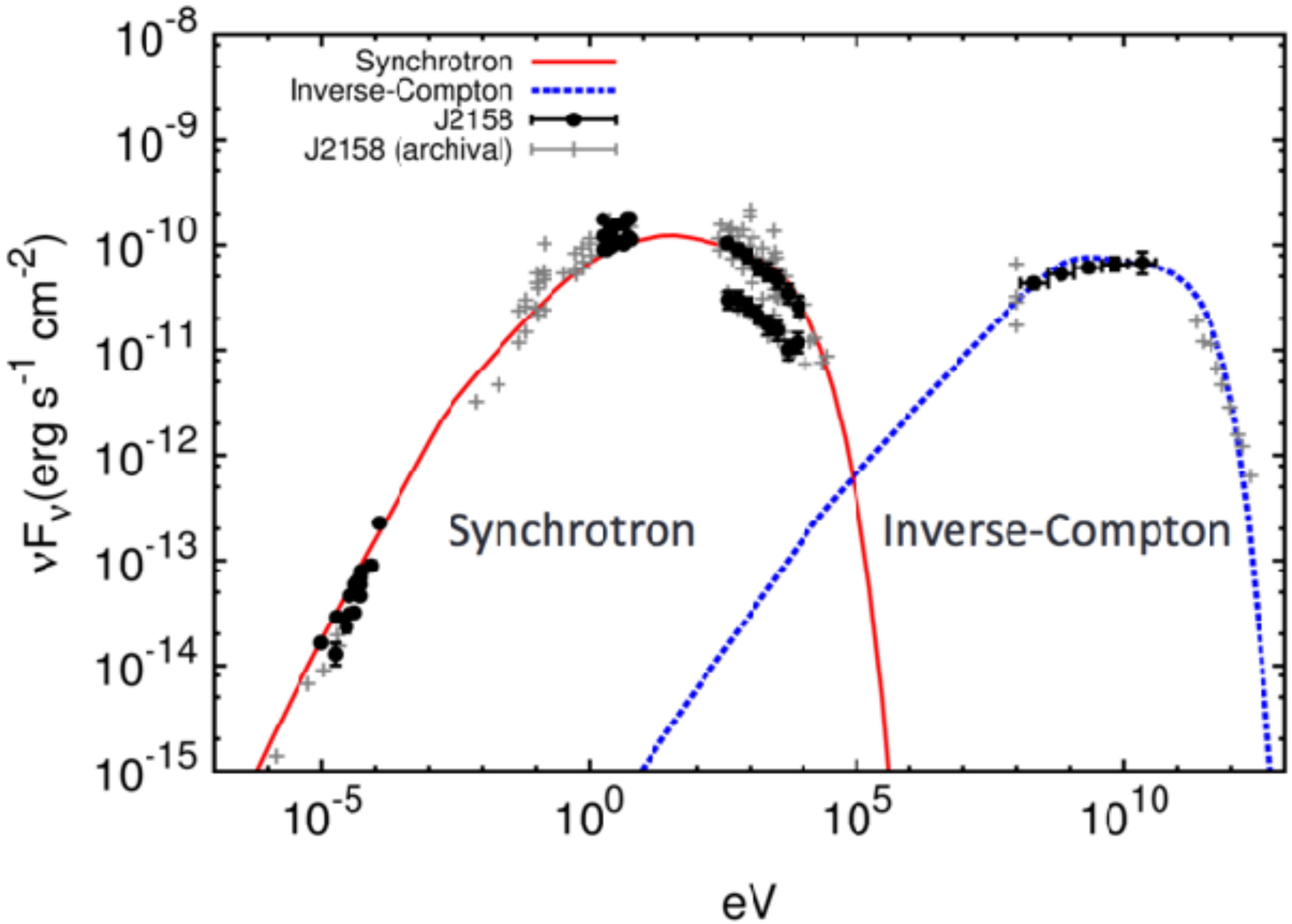

Nieppola et al. 2006, A&A, 445, 441

- **Calculated SEDs for 308 BL Lacs and set roughly boundary as:**

$$LBLs: \quad \log \nu_p < 14.5$$

$$IBLs: \quad 14.5 < \log \nu_p < 16.5$$

$$HBLs: \quad \log \nu_p > 16.5$$

L: Lower, I: Intermediate, H: High

Abdo et al. 2010, ApJ, 715, 429

- **Calculated SEDs for 80 blazars and set roughly boundary as:**

$$LSPs: \quad \log \nu_p < 14$$

$$ISPs: \quad 14 < \log \nu_p < 15$$

$$HSPs: \quad \log \nu_p > 15$$

Lower, Intermediate, High Synchrotron Peak

Fan, Yang, Pei et al. 2016, ApJS, 226, 20

- **Calculating SEDs for 1425 Fermi blazars from 3FGL and using multi-wavelengh flux density by fitting**

$$\log \nu F_{\nu} = P_1 (\log \nu - P_2)^2 + P_3$$

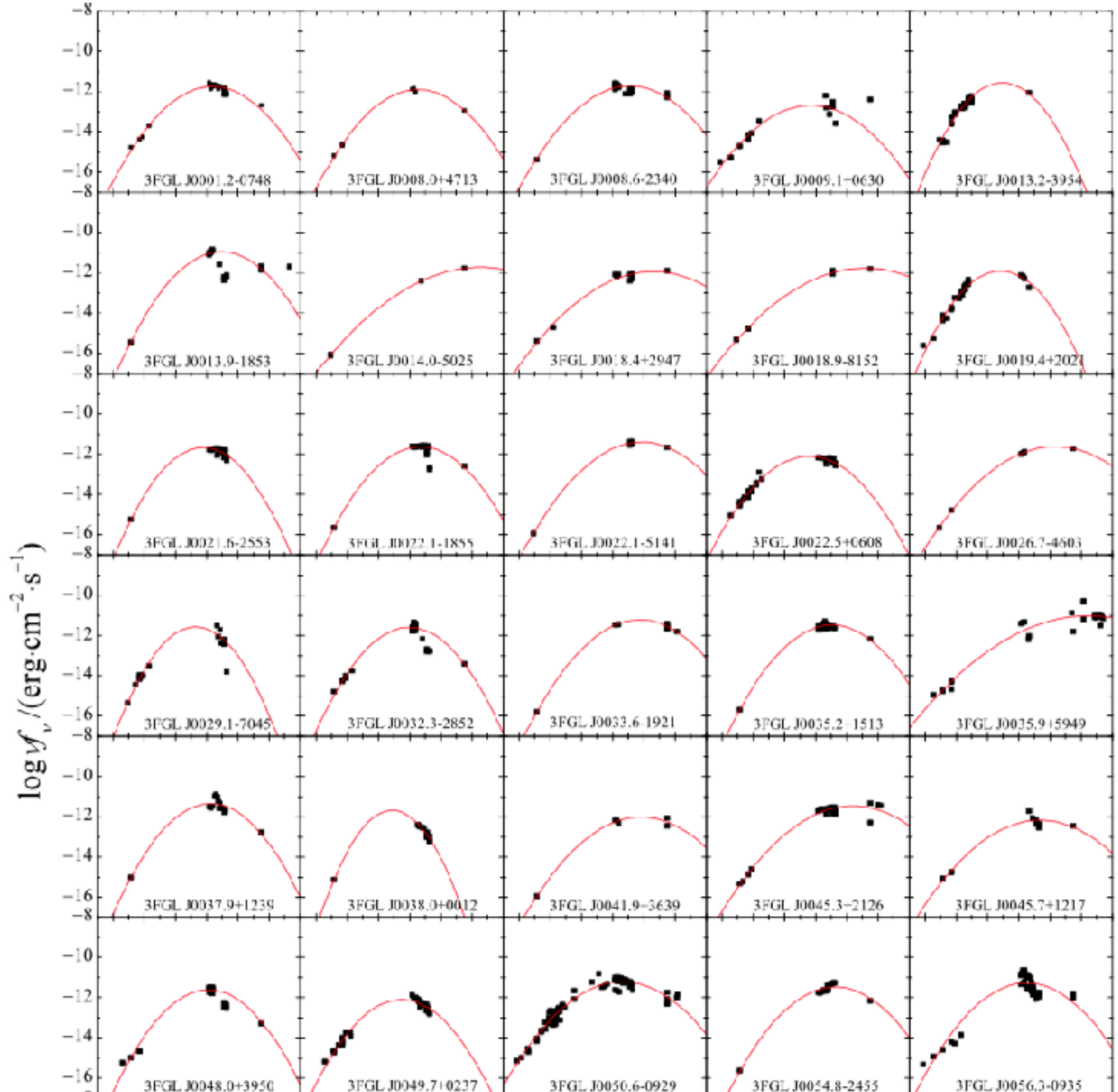

log νf_ν /(erg·cm^-2·s^-1)
3FGL J0001.2-0748
3FGL J0008.0+4713
3FGL J0008.6-2340
3FGL J0009.1-0630
3FGL J0013.2-3954
3FGL J0013.9-1853
3FGL J0014.0-5025
3FGL J0018.4+2947
3FGL J0018.9-8152
3FGL J0019.4+2021
3FGL J0021.6-2553
3FGL J0022.1-1855
3FGL J0022.1-5141
3FGL J0022.5+0608
3FGL J0026.7-4603
3FGL J0029.1-7045
3FGL J0032.3-2852
3FGL J0033.6-1921
3FGL J0035.2-1513
3FGL J0035.9+5949
3FGL J0037.9+1239
3FGL J0038.0+0012
3FGL J0041.9-3639
3FGL J0045.3-2126
3FGL J0045.7+1217
3FGL J0048.0+3950
3FGL J0049.7+0237
3FGL J0050.6-0929
3FGL J0054.8-2455
3FGL J0056.3-0935

Sample for Blazars

3FGL Name	z	C	L_R/σ_{L_R}	L_O/σ_{L_O}	L_X/σ_{L_X}	$L_\gamma/\sigma_{L_\gamma}$	$\alpha_{RO}/\sigma_\alpha$	$\alpha_{OX}/\sigma_\alpha$	P_1/σ_{P_1}	ν_p/σ_{ν_p}	L_p/σ_{L_p}	$L_{bol}/\sigma_{L_{bol}}$
(1)	(2)	(3)	(4)	(5)	(6)	(7)	(8)	(9)	(10)	(11)	(12)	(13)
J0001.2-0748	⋯	IB	42.36/0.01	45.39/0.02	⋯	45.23/0.06	0.45/0.01	⋯	−0.12/0.01	14.37/0.12	45.35/0.03	45.71/0.05
J0001.4+2120	1.106	HF	42.97/0.01	⋯	⋯	45.70/0.11	⋯	⋯	−0.05/0.00	16.79/0.28	45.70/0.03	46.32/0.04
J0003.2-5246	⋯	HU	⋯	⋯	45.13/0.07	44.56/0.11	⋯	⋯	−0.05/0.01	17.89/0.81	45.15/0.14	45.76/0.14
J0003.8-1151	1.310	LU	43.44/0.01	45.54/0.04	⋯	45.59/0.12	0.62/0.01	⋯	−0.12/0.01	13.06/0.14	45.57/0.11	46.01/0.15
J0004.7-4740	0.880	IF	⋯	46.38/0.04	44.98/0.07	45.86/0.05	⋯	1.52/0.04	−0.12/0.01	14.14/0.09	46.20/0.06	46.59/0.09
J0006.4+3825	0.229	IF	41.98/0.01	44.53/0.04	43.44/0.07	44.41/0.06	0.54/0.01	1.40/0.04	−0.11/0.01	14.03/0.12	44.65/0.10	45.08/0.14
J0008.0+4713	0.280	IB	41.18/0.01	⋯	43.51/0.07	44.87/0.03	⋯	⋯	−0.12/0.00	14.52/0.07	44.46/0.04	44.83/0.06
J0008.6-2340	0.147	IB	40.38/0.01	⋯	43.72/0.05	43.08/0.12	⋯	⋯	−0.10/0.01	15.09/0.19	44.01/0.05	44.40/0.07
J0009.1+0630	⋯	LB	42.43/0.02	44.97/0.04	⋯	45.14/0.07	0.54/0.01	⋯	−0.09/0.03	13.69/0.51	44.42/0.17	44.93/0.24
J0009.6-3211	0.026	LU	39.87/0.01	44.48/0.04	41.53/0.13	41.91/0.10	0.17/0.01	2.09/0.06	−0.16/0.02	13.93/0.24	43.90/0.17	44.14/0.23
J0013.2-3954	⋯	LB	42.74/0.02	45.04/0.04	⋯	45.21/0.06	0.58/0.01	⋯	−0.19/0.01	12.95/0.14	45.53/0.09	45.79/0.13
J0013.9-1853	0.095	IB	39.90/0.02	⋯	43.72/0.03	42.88/0.11	⋯	⋯	−0.13/0.01	14.96/0.15	44.37/0.07	44.65/0.09
J0014.0-5025	⋯	HB	⋯	⋯	45.38/0.07	44.64/0.10	⋯	⋯	−0.05/0.00	18.55/0.33	45.38/0.06	45.94/0.07
J0015.7+5552	⋯	HU	41.90/0.01	⋯	⋯	44.93/0.09	⋯	⋯	−0.10/0.00	15.82/0.10	45.95/0.03	46.32/0.04
J0016.3-0013	1.577	IF	43.96/0.01	45.49/0.04	45.02/0.07	46.67/0.06	0.72/0.01	1.17/0.04	−0.09/0.01	13.58/0.10	45.58/0.04	46.12/0.06
J0017.2-0643	⋯	IU	41.94/0.01	44.82/0.04	⋯	44.87/0.09	0.48/0.01	⋯	−0.10/0.01	14.64/0.37	44.79/0.06	45.21/0.09
J0017.6-0512	0.227	IF	41.46/0.02	44.30/0.04	43.78/0.11	44.48/0.05	0.49/0.01	1.19/0.05	−0.11/0.01	14.48/0.13	44.63/0.15	45.02/0.21
J0018.4+2947	0.100	HB	40.00/0.01	⋯	43.54/0.07	42.84/0.13	⋯	⋯	−0.06/0.01	16.60/0.68	43.44/0.12	43.96/0.16
J0018.9-8152	⋯	HB	⋯	⋯	45.37/0.09	45.16/0.06	⋯	⋯	−0.05/0.01	17.16/0.46	45.33/0.07	45.90/0.07
J0019.1-5645	⋯	LU	⋯	⋯	⋯	44.88/0.09	⋯	⋯	−0.13/0.01	13.35/0.10	44.04/0.06	44.41/0.10
J0019.4+2021	⋯	LB	43.04/0.01	44.42/0.04	⋯	44.91/0.10	0.75/0.01	⋯	−0.17/0.01	12.84/0.09	45.19/0.06	45.50/0.10
J0021.6-2553	⋯	LB	41.88/0.01	45.06/0.14	⋯	45.14/0.06	0.43/0.03	⋯	−0.17/0.02	13.77/0.17	45.43/0.08	45.67/0.12
J0021.6-6835	⋯	IU	⋯	⋯	44.82/0.08	44.87/0.12	⋯	⋯	−0.09/0.01	14.90/0.13	45.47/0.04	45.92/0.05
J0022.1-1855	⋯	IB	41.39/0.02	45.60/0.02	44.56/0.11	45.13/0.05	0.24/0.01	1.38/0.05	−0.13/0.01	14.69/0.12	45.46/0.03	45.76/0.05
J0022.1-5141	⋯	HB	⋯	⋯	45.51/0.07	45.14/0.05	⋯	⋯	−0.09/0.00	15.86/0.16	45.69/0.03	46.07/0.05
J0022.5+0608	⋯	LB	42.57/0.01	44.64/0.04	⋯	45.68/0.03	0.63/0.01	⋯	−0.12/0.01	13.58/0.12	45.00/0.06	45.40/0.09

Monochromatic Luminosity

Effective spectral index

Fitting Results P1,P2,P3

Fan, Yang, Pei et al. 2016, ApJS, 226, 20

$$LSPs: \log \nu_p \le 14.0$$

$$ISPs: 14.0 < \log \nu_p \le 15.3$$

$$HSPs: \log \nu_p > 15.3$$

The results are similar to those by Abdo et al. 2010

1.2 Relativistic Beaming Effect

1.2 Relativistic Beaming Effect

Beaming factor: $$\delta = \frac{1}{\gamma(1-\beta\cos\theta)}$$

Lorentz factor: $$\gamma = \frac{1}{1-\beta^2},\ \beta = \frac{v}{c}$$

1.2 Relativistic Beaming Effect

Beaming factor: $$\delta = \frac{1}{\gamma(1-\beta\cos\theta)}$$

Lorentz factor: $$\gamma = \frac{1}{1-\beta^2},\ \beta = \frac{v}{c}$$

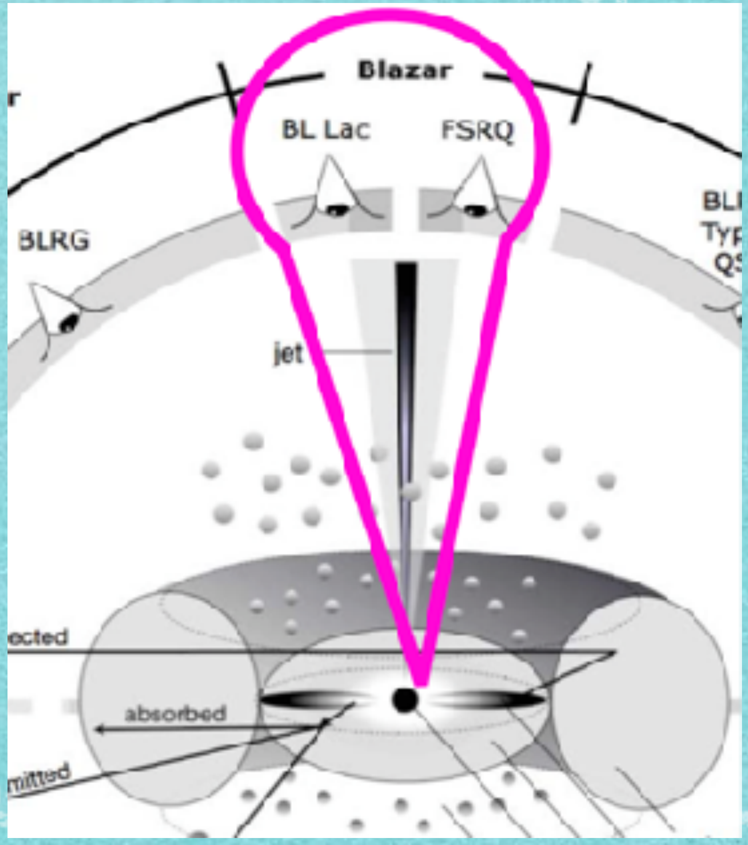

1.2 Relativistic Beaming Effect

$$S_{obs} = \delta^{p} \cdot S_{in}$$

$p = 2 + \alpha$

continuous jet

$p = 3 + \alpha$

moving sphere

Outline

- 1. Introduction to Active Galactic Nuclei and Beaming Effect;
- 2. Fermi Large Area Telescope;
- 3. Core Dominance Parameter and Data Analysis;
- 4. Relationship between Spectral Index and Core Dominance Parameter;
- 5. Summary and Discussion.

2. Fermi / LAT

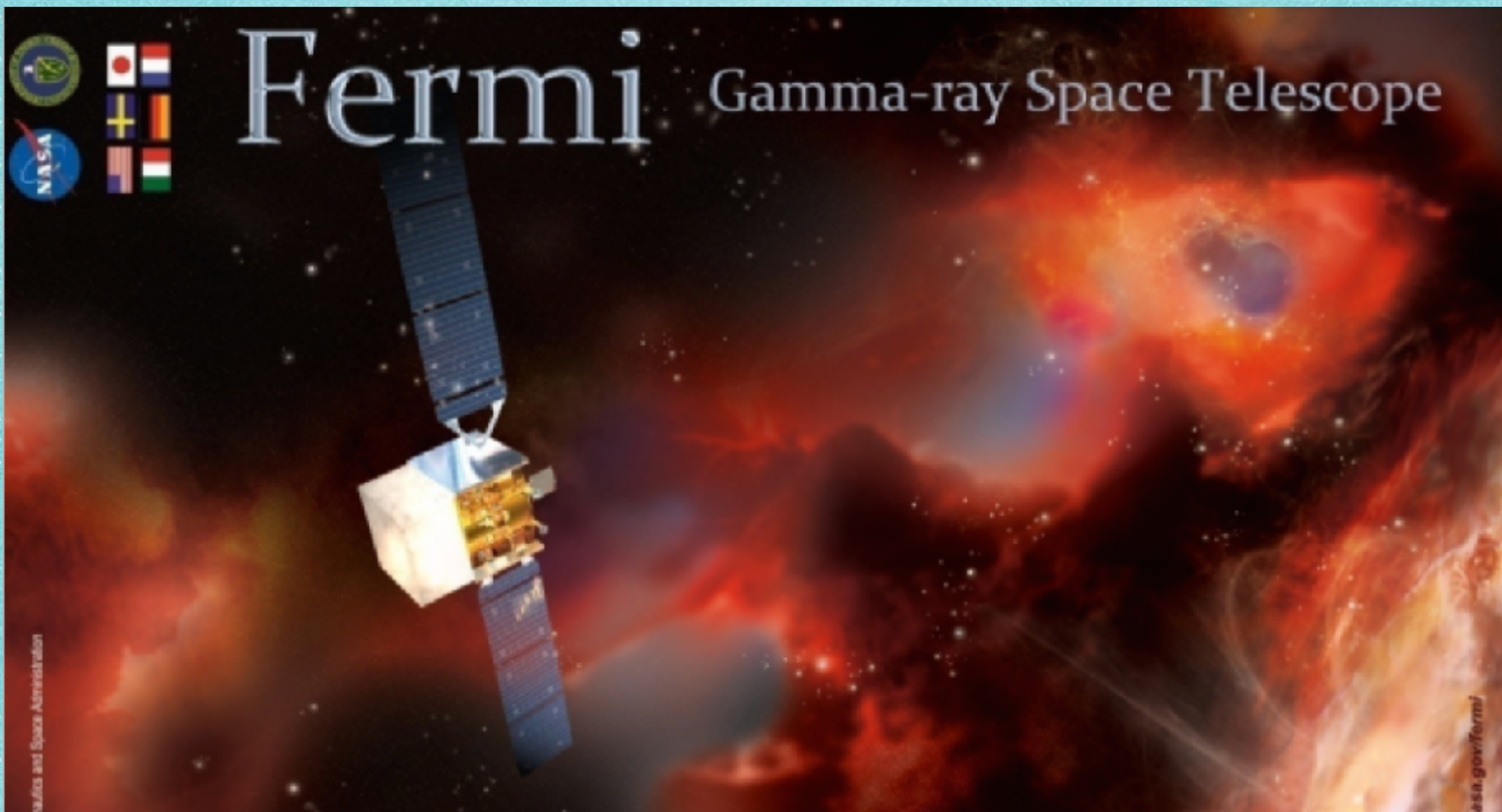

2. Fermi / LAT

Launching in June 11, 2008!

十年啦！

Ten years!

Dieci anni!

The Fermi era

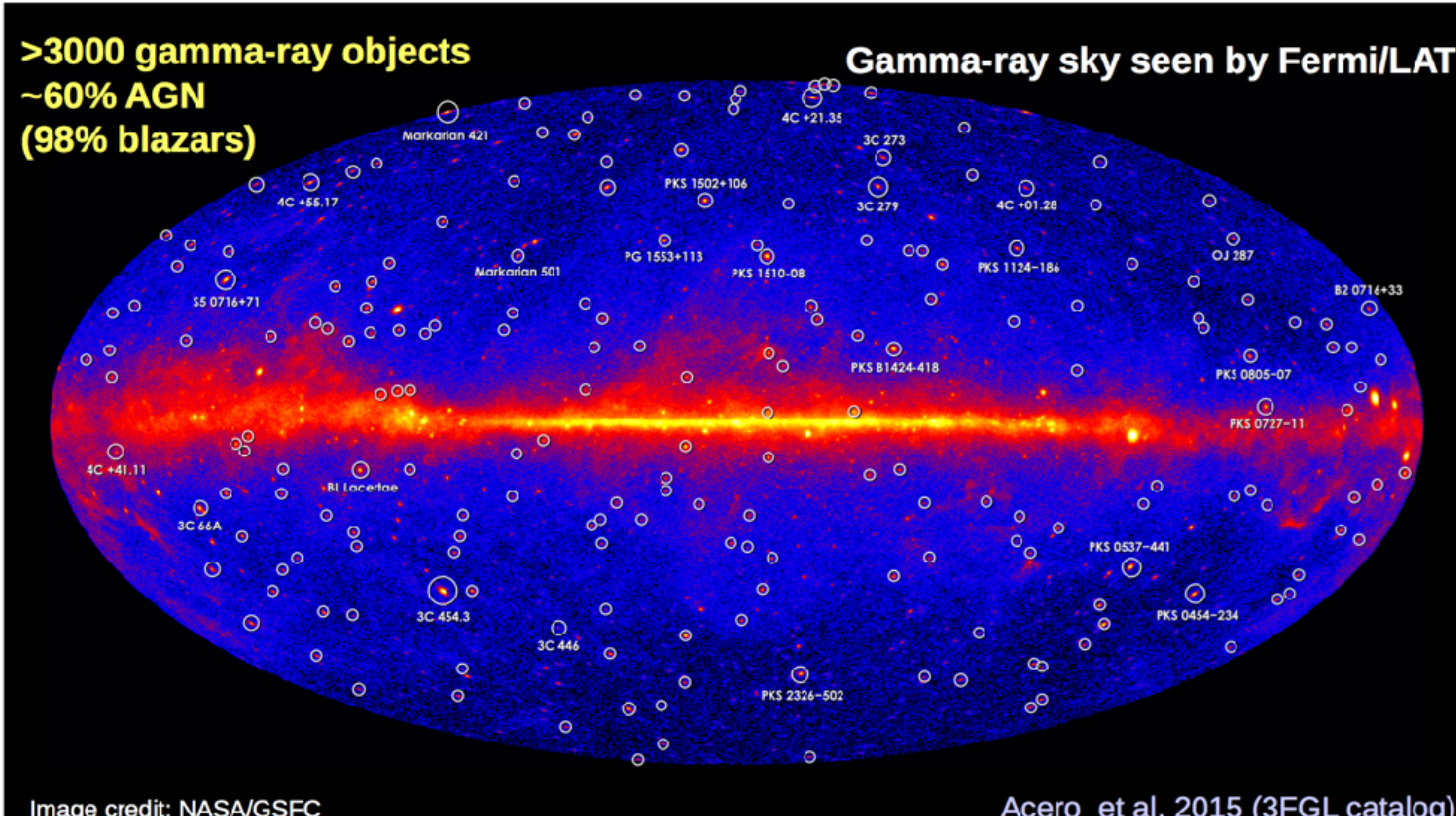

Since its launch in 2008, the **Fermi-LAT (Large Area Telescope)** has revolutionized our knowledge of gamma-ray sky with a combination of **high sensitivity, wide field-of-view, and large energy range (about 20 MeV to more than 300 GeV)**.

Celebrating 10 Years of Fermi

June 11, 2018

Data

- Data Policy
- Data Access
  - + LAT Data
  - + LAT Catalog
  - + LAT Data Queries
  - + LAT Query Results
  - + LAT Weekly Files
  - + GBM Data
- Data Analysis
- Caveats
- Newsletters
- FAQ

Preliminary LAT 8-year Point Source List (FL8Y)

This page provides a preliminary Fermi Large Area Telescope (LAT) list of sources (FL8Y) initially meant to help in writing 2018 NASA Fermi Guest Investigator proposals. Based on the first eight years of science data from the Fermi Gamma-ray Space Telescope mission and the 100 MeV-1 TeV range, it is the deepest yet in this energy range. Relative to the 3FGL catalog, the FL8Y source list has twice as much exposure as well as a number of analysis improvements, but is lacking an updated model for Galactic diffuse gamma-ray emission. The FL8Y source list includes 5523 sources above 4-sigma significance, with source location regions and spectral properties. Fifty-eight sources are modeled explicitly as spatially extended, and overall 300 sources are considered as identified based on angular extent or correlated variability (periodic or otherwise) observed at other wavelengths. For 2131 sources we have not found plausible counterparts at other wavelengths. More than 2900 of the identified or associated sources are active galaxies of the blazar class, 218 are pulsars. This source list is meant to be replaced within a few months by the official 4FGL catalog which will benefit from an improved model of diffuse emission.

Caveats

The FL8Y list is meant to provide researchers analyzing Fermi data with an updated description of the gamma-ray sky with respect to 3FGL. It contains nearly 2500 new sources which can be used as a starting point for new works. It can also be used for modelling the source background in a region of interest.

Being a courtesy effort, FL8Y is neither published nor posted on the arXiv. We request the community users to refrain from publishing works (in particular population studies) using directly material from FL8Y, and wait for the future 4FGL catalog that will supersede FL8Y.

FL8Y Source List Data Products

The 8-year Source List is currently available as a FITS file. Supporting tools and documentation have been provided and are linked below.

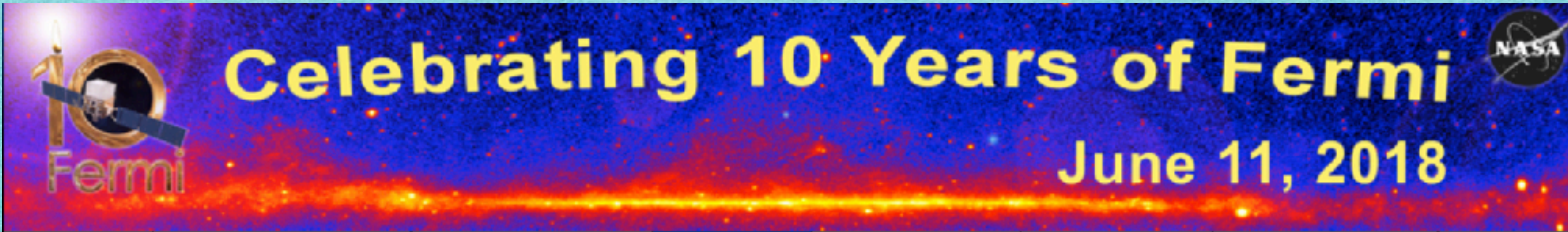

Preliminary LAT 8-year Point Source List (FL8Y)

This page provides a preliminary Fermi Large Area Telescope (LAT) list of sources (FL8Y) initially meant to help in writing 2018 NASA Fermi Guest Investigator proposals. Based on the first eight years of science data from the Fermi Gamma-ray Space Telescope mission and the 100 MeV-1 TeV range, it is the deepest yet in this energy range. Relative to the 3FGL catalog, the FL8Y source list has twice as much exposure as well as a number of analysis improvements, but is lacking an updated model for Galactic diffuse gamma-ray emission. The FL8Y source list includes 5523 sources above 4-sigma significance, with source location regions and spectral properties. Fifty-eight sources are modeled explicitly as spatially extended, and overall 300 sources are considered as identified based on angular extent or correlated variability (periodic or otherwise) observed at other wavelengths. For 2131 sources we have not found plausible counterparts at other wavelengths. More than 2900 of the identified or associated sources are active galaxies of the blazar class, 218 are pulsars. This source list is meant to be replaced within a few months by the official 4FGL catalog which will benefit from an improved model of diffuse emission.

5523 sources

Caveats

The FL8Y list is meant to provide researchers analyzing Fermi data with an updated description of the gamma-ray sky with respect to 3FGL. It contains nearly 2500 new sources which can be used as a starting point for new works. It can also be used for modelling the source background in a region of interest.

Being a courtesy effort, FL8Y is neither published nor posted on the arXiv. We request the community users to refrain from publishing works (in particular population studies) using directly material from FL8Y, and wait for the future 4FGL catalog that will supersede FL8Y.

FL8Y Source List Data Products

The 8-year Source List is currently available as a FITS file. Supporting tools and documentation have been provided and are linked below.

2.1 LAT FL8Y Blazars

BL Lacs	1008
FSRQs	618
BCUs	1229

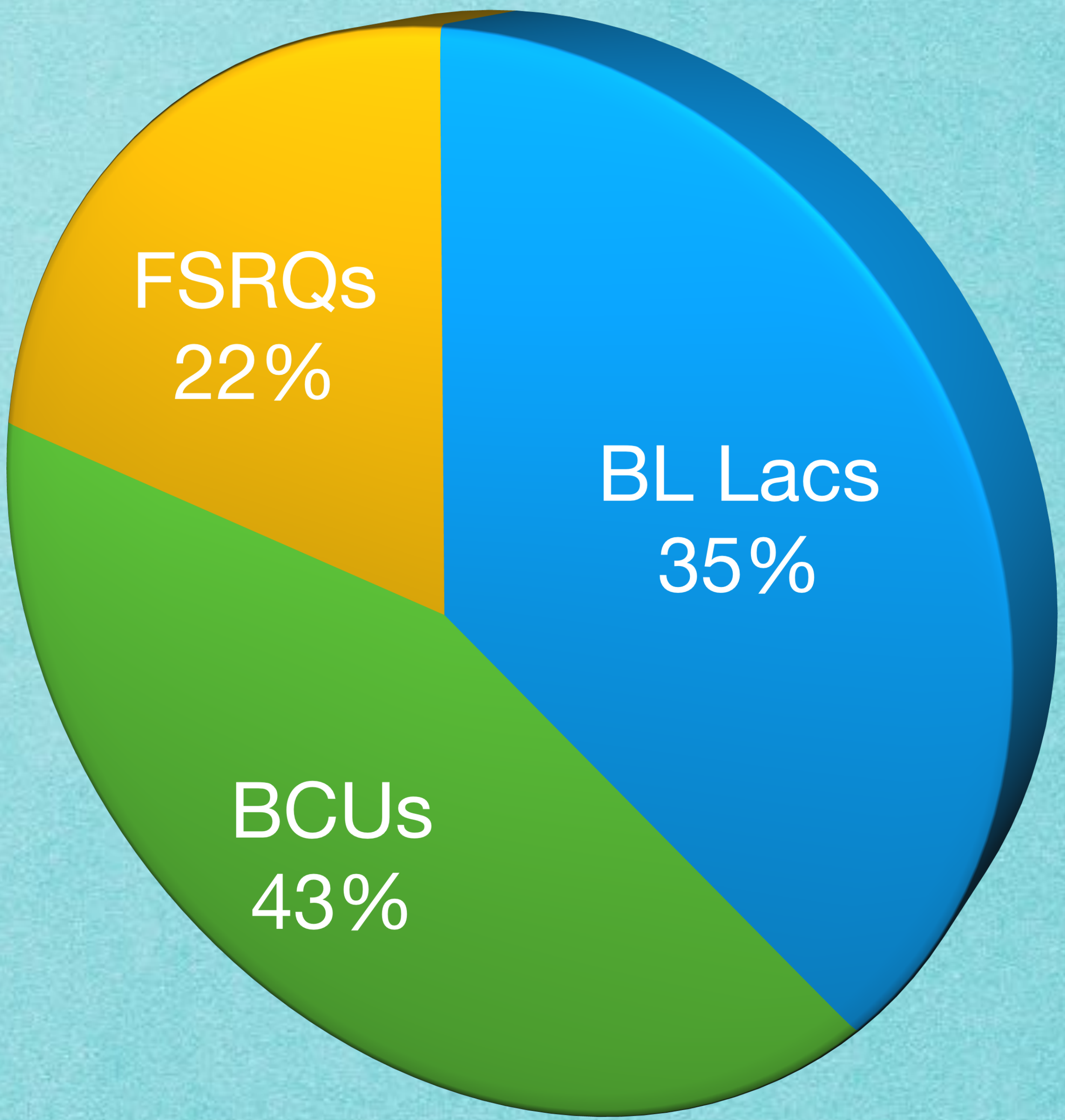

Outline

- 1. Introduction to Active Galactic Nuclei and Beaming Effect;
- 2. Fermi Large Area Telescope;
- **3. Core-Dominance Parameter and Data Analysis;**
- 4. Correlation between Spectral Index and Core-Dominance Parameter;
- 5. Summary and Discussion.

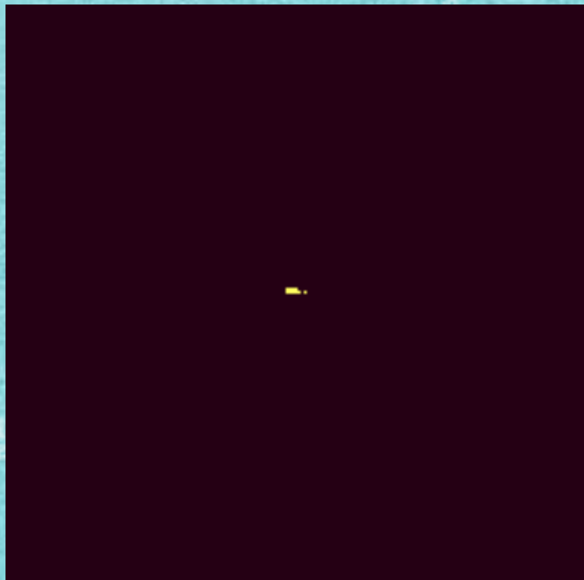

3.1 Core-Dominance Parameter

The radio emissions are consisted of two components, namely the core and the extended emissions.

3.1 Core–Dominance Parameter

The emissions are consisted of two components, namely the core and the extended emissions.

$$R = \frac{S_{core}}{S_{extend}}$$

R: Core-Dominance Parameter

3.1 Core-Dominance Parameter

or we can take,

$$R = \frac{L_{core}}{L_{extend}}$$

3.1 Core-Dominance Parameter

$$S_{core}^{5GHz} = S_{core}^{\nu,obs}, \quad S_{ext.}^{5GHz} = S_{ext.}^{\nu,obs} \left(\frac{\nu}{5GHz}\right)^{\alpha_{ext.}}$$

$$\log R = \log\left(\frac{S_{core}}{S_{ext.}}\right)(1+z)^{\alpha_{core}-\alpha_{ext.}}$$

we take:

$$\alpha_{core} = 0.00, \alpha_{ext.} = 0.75$$

(Fan et al. 2011, Pei et al. 2016; 2018, in prep)

3.1 Core-Dominance Parameter

$$R = f\delta^{3+\alpha}(or\ \ f\delta^{2+\alpha})$$

(Ghisellini et al. 1993)

$$R = f\{[\gamma(1-\beta\cos\theta)]^{-3} + [\gamma(1+\beta\cos\theta)]^{-3}\}$$

(Urry and Padovani 1995)

3.2 Previous work

Basing on 3FGL, we compiled **1335** objects with available core-dominance parameter, **log R**, which consisted of **169** ***Fermi-Detected Blazars*** (***FBs***) and **1166** ***non-Fermi-Detected Blazars*** (***non-FBs***).

(Pei et al. 2016, ApSS, 361, 237)

3.2 Previous work

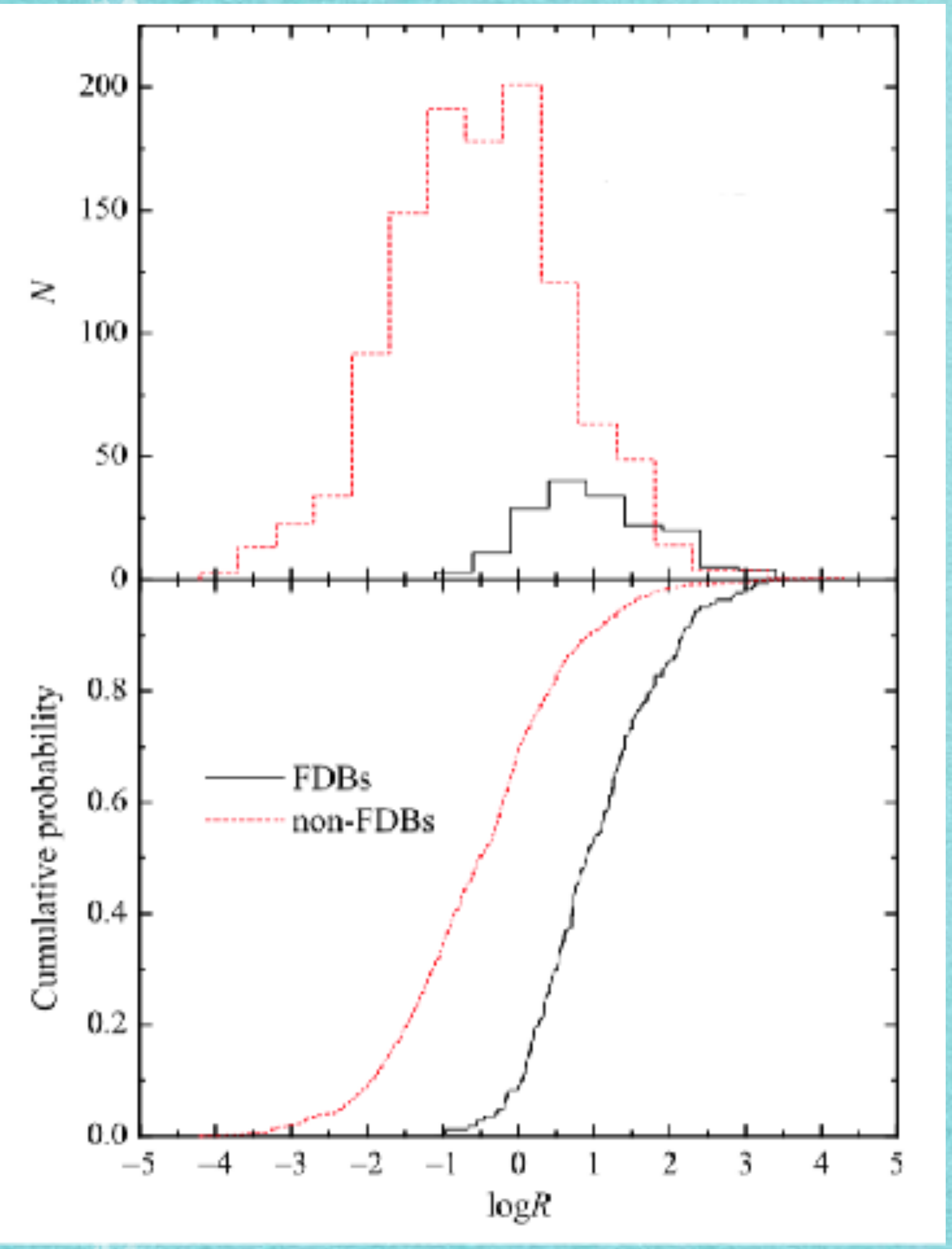

FBs : $< \log R > \simeq 0.99$

non-FBs : $< \log R > \simeq -0.62$

(Pei et al. 2016, ApSS, 361, 237)

3.2 Previous work

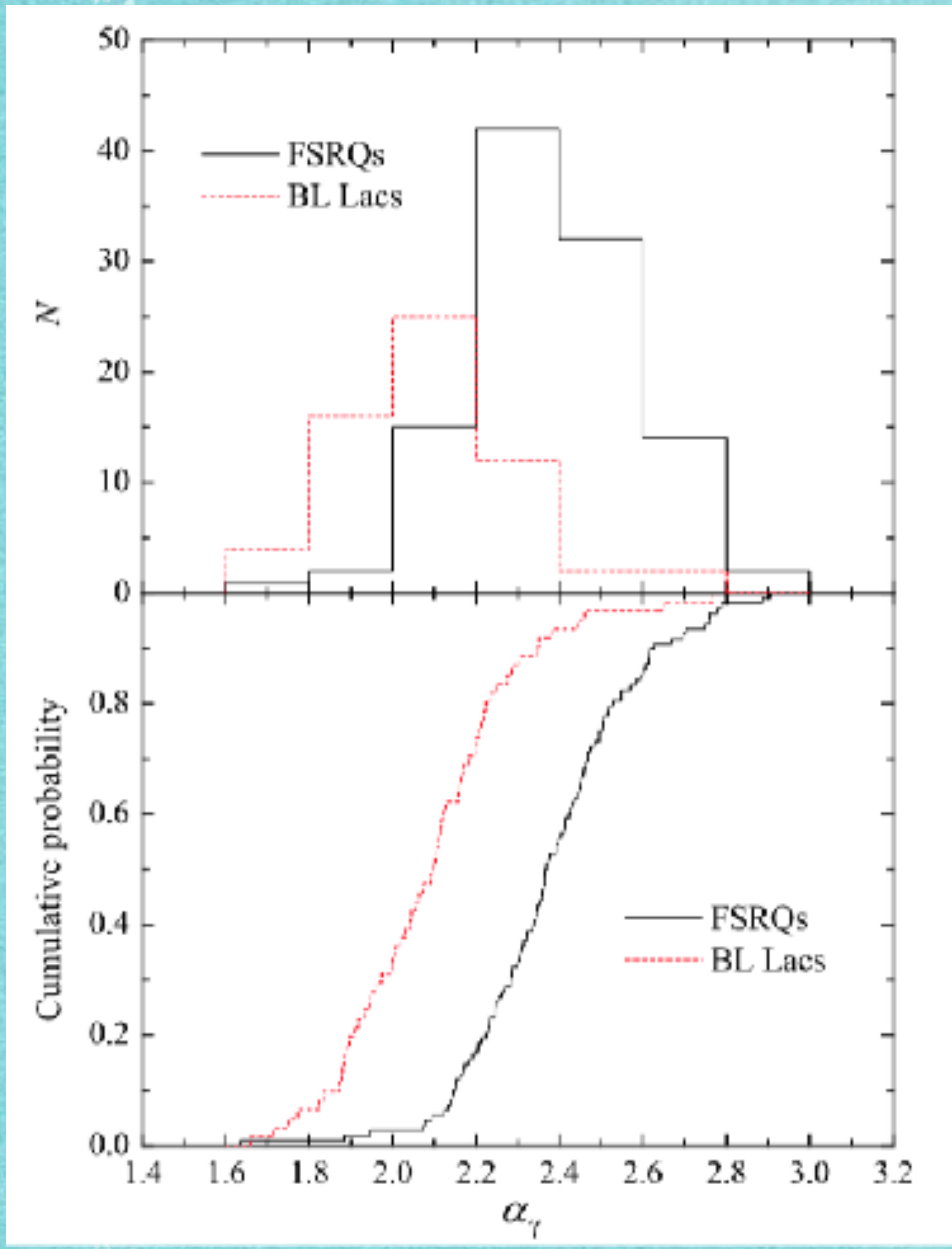

BL Lacs : $< \alpha_\gamma > \simeq 2.10$

FSRQs : $< \alpha_\gamma > \simeq 2.38$

(Pei et al. 2016, ApSS, 361, 237)

3.3 Recent

Basing on FL8Y, we compiled **626** ***Fermi blazars*** and **1031** ***non-Fermi blazars*** with available core-dominance parameter **(log R)**, consisted of **270** ***BL Lacs, 302 FSRQs*** and 54 ***BCUs***. We use these data to study the **beaming effect** and **radio dominance of** Fermi blazars.

(Pei et al. 2018, in prep)

3.4 Comparison of logR between FBs and non-FBs

$$\text{FBs} : \langle \log \mathrm{R} \rangle \simeq 0.630$$
$$\text{non-FBs} : \langle \log \mathrm{R} \rangle \simeq -0.439$$

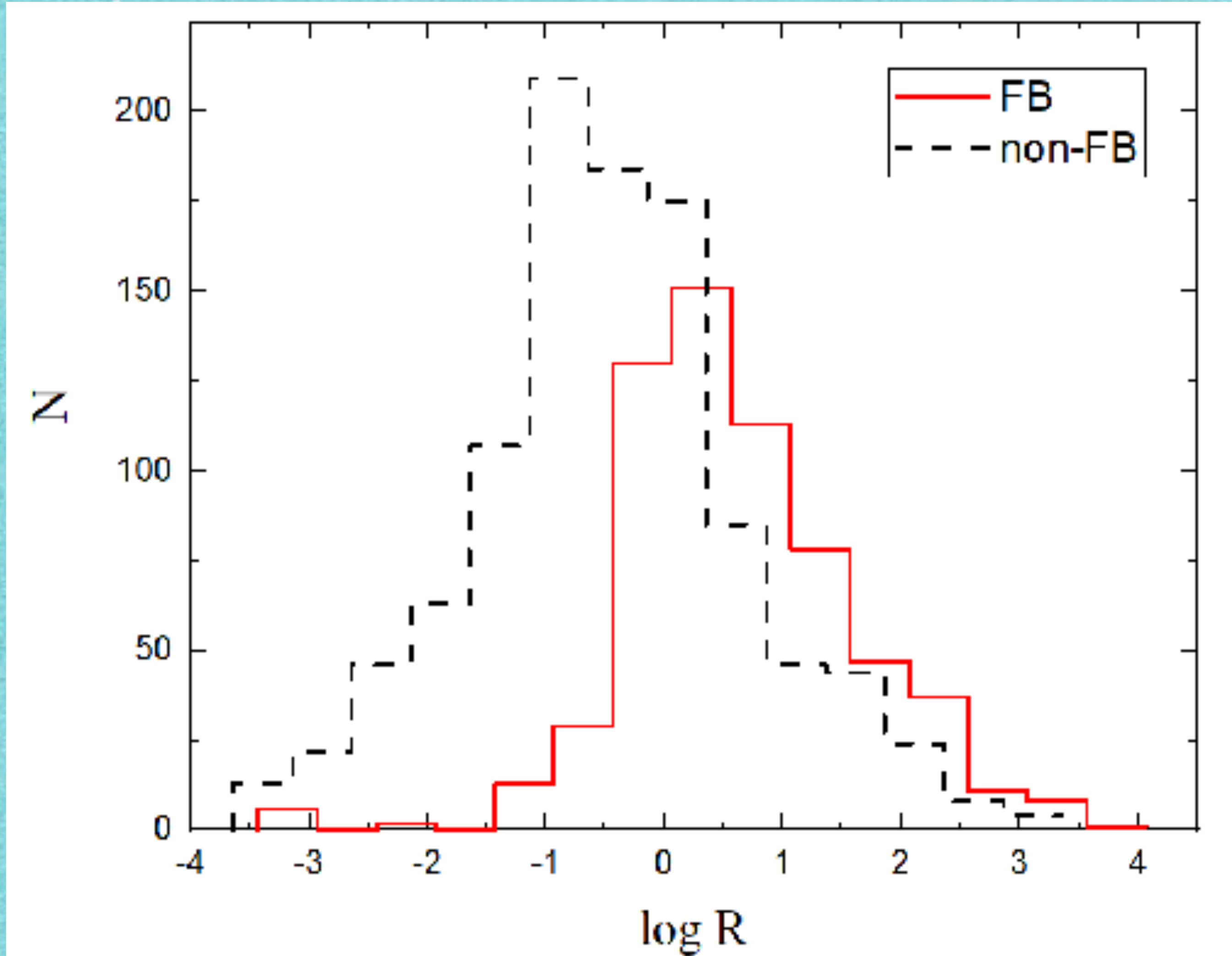

Preliminary

Histogram

Cum-Prob

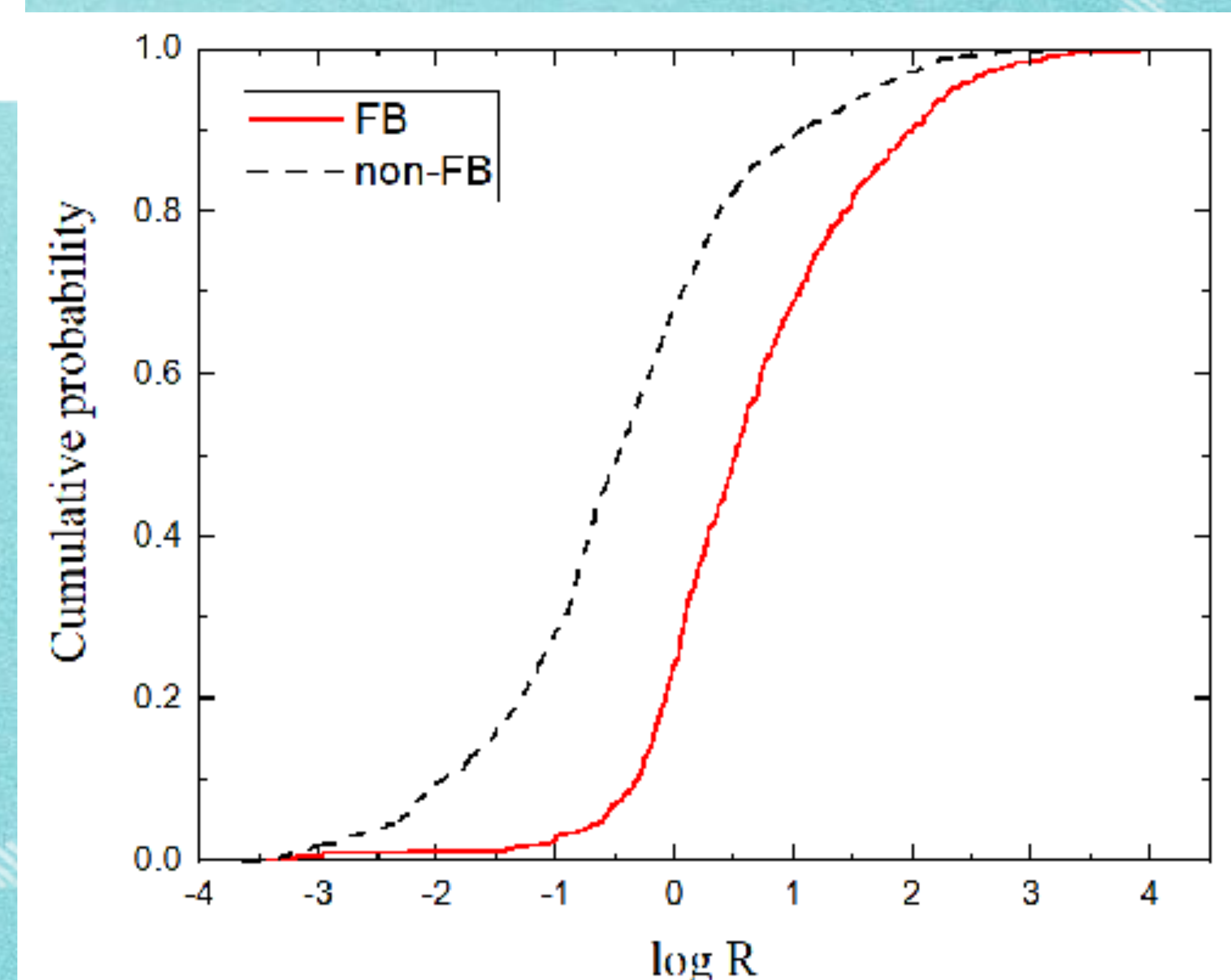

K-S test:

$$p = 8.064 \times 10^{-75}$$

3.4 Comparison of logR in FBs

$$\text{BL Lacs} : < \log \mathrm{R} > \simeq 0.669$$
$$\text{FSRQs} : < \log \mathrm{R} > \simeq 0.703$$
$$\text{BCUs} : < \log \mathrm{R} > \simeq 0.026$$

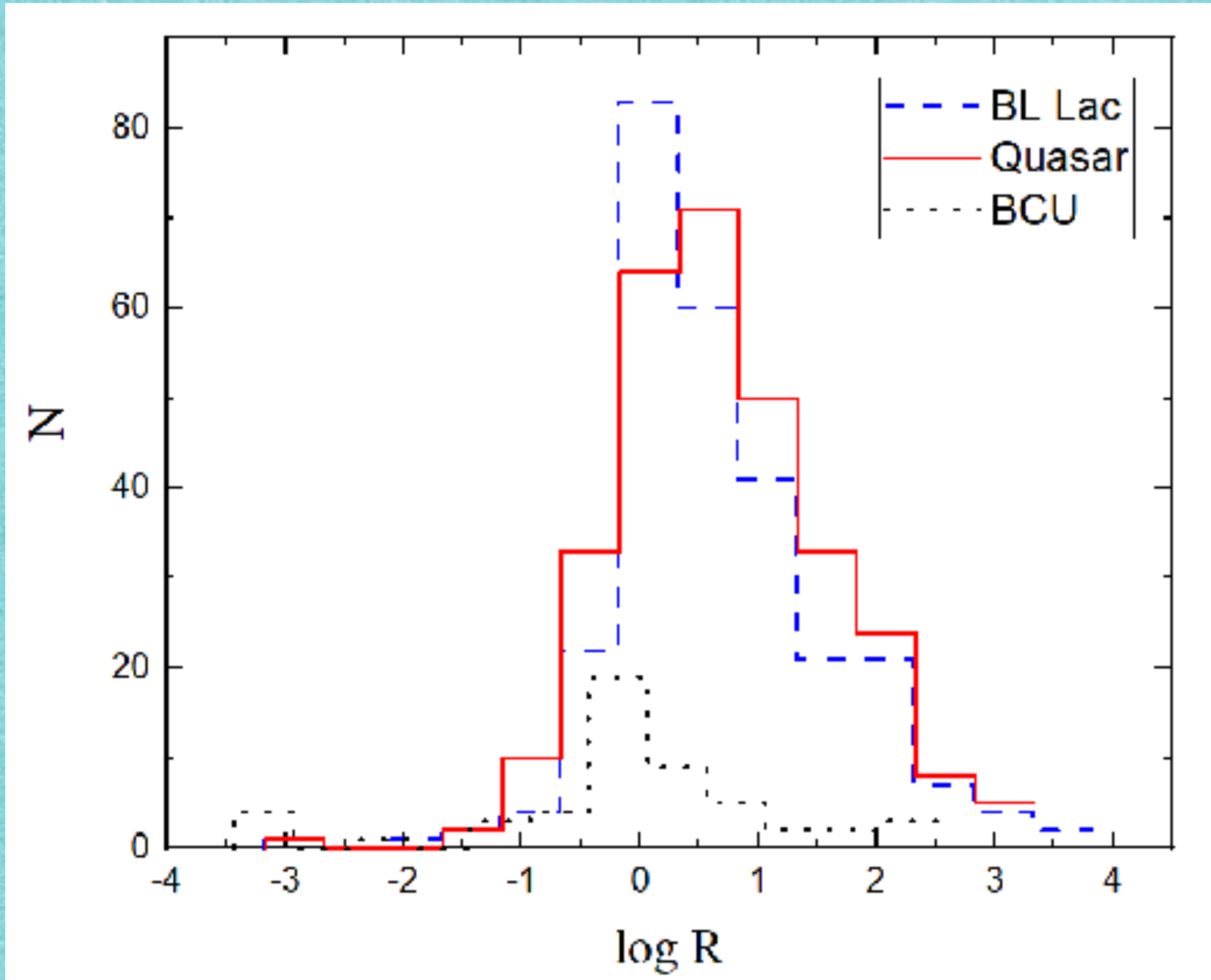

Histogram

Preliminary

Cum-Prob

K-S test for BL Lacs and FSRQs:

$$p = 0.281$$

Not significant different!

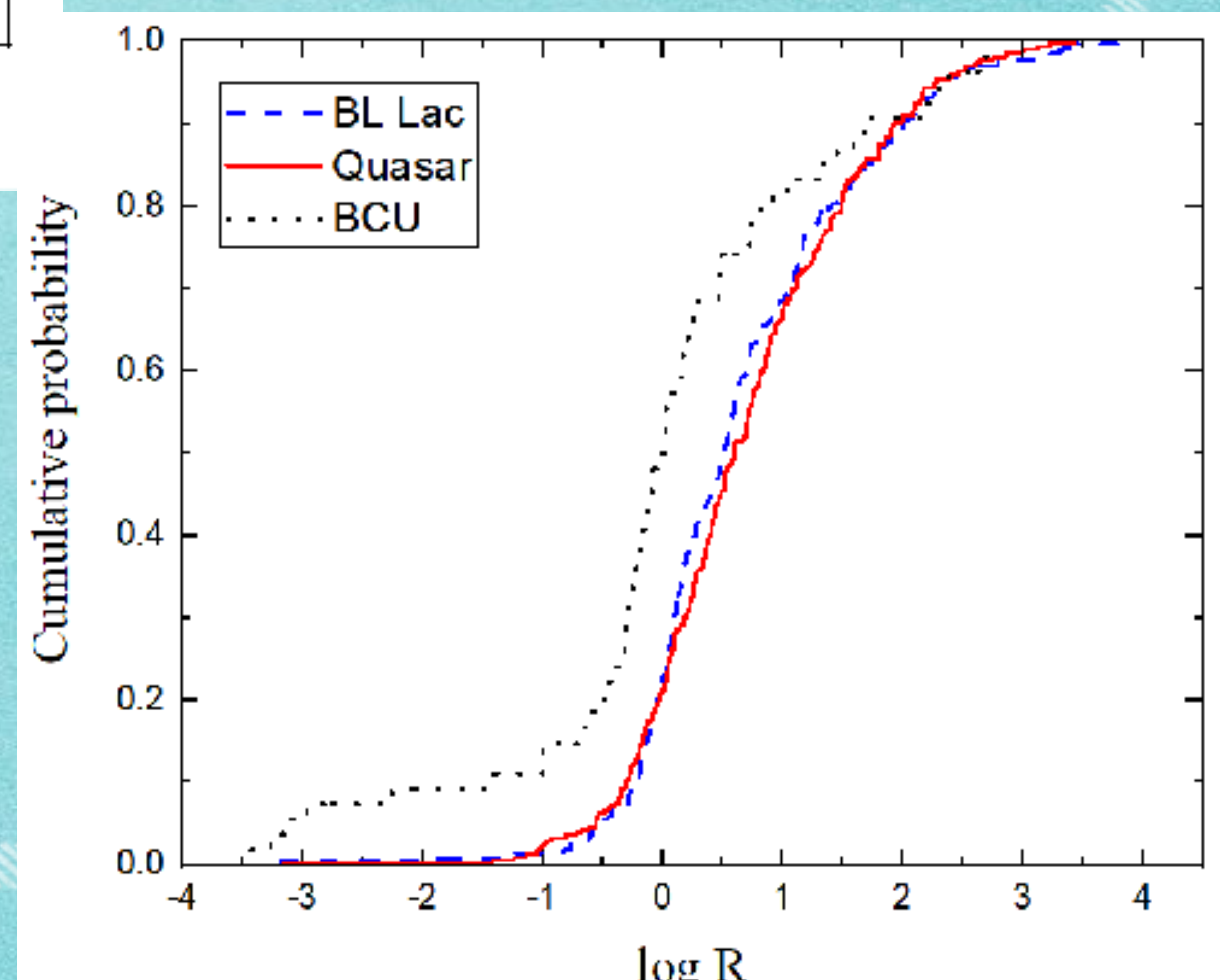

- The averaged of logR for FBs is higher than those for non-FBs.

3.5 Comparison of Gamma-Ray Spectral Index in FBs

$$<\alpha_\gamma>|_{BL\ Lacs} \simeq 2.04$$

$$<\alpha_\gamma>|_{FSRQs} \simeq 2.50$$

$$<\alpha_\gamma>|_{BCUs} \simeq 2.30$$

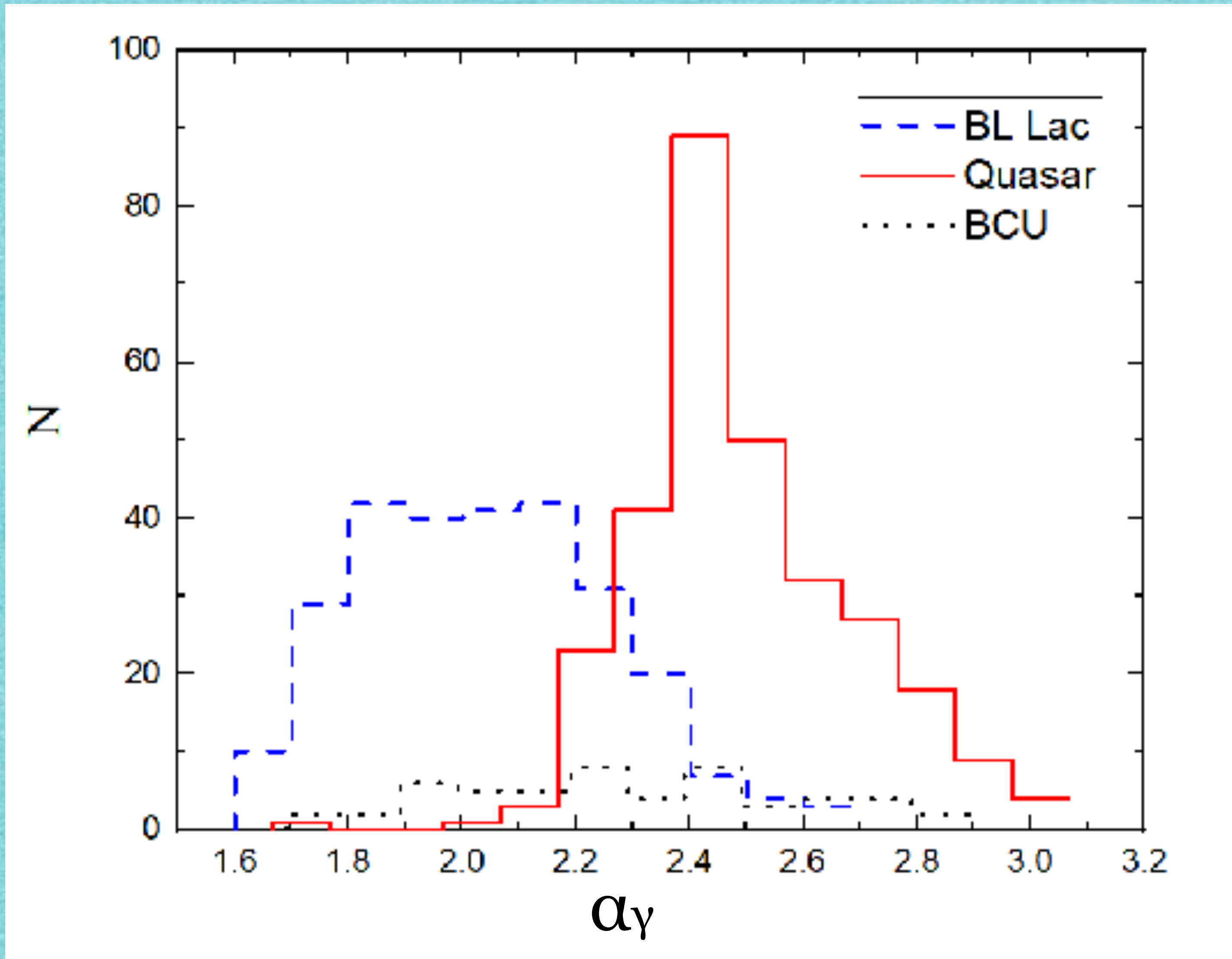

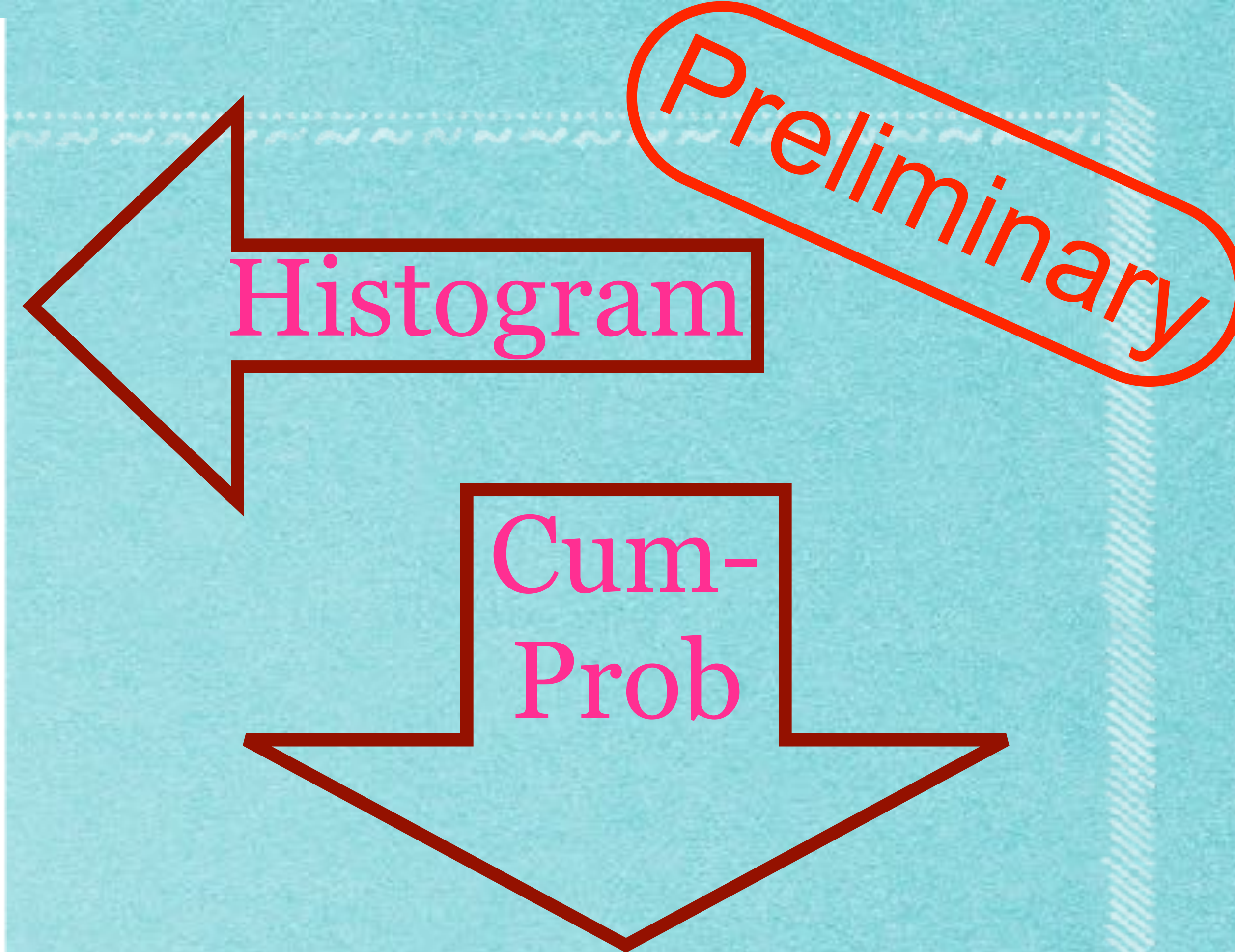

K-S test for BL Lacs and FSRQs:

$$p = 5.169 \times 10^{-72}$$

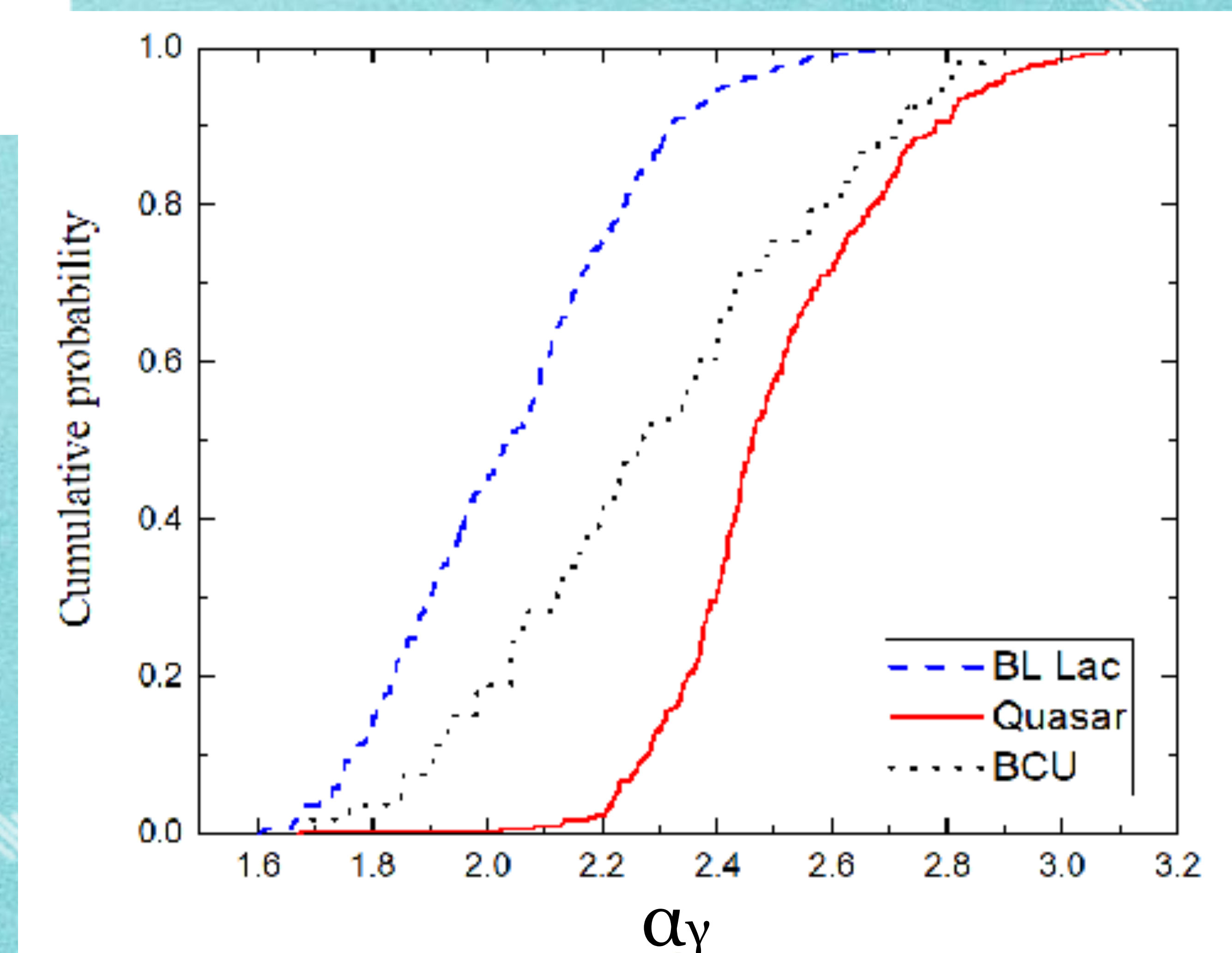

Outline

- 1. Introduction to Active Galactic Nuclei and Beaming Effect;
- 2. Fermi Large Area Telescope;
- 3. Core-Dominance Parameter and Data Analysis;
- **4. Correlation between Spectral Index and Core-Dominance Parameter;**
- 5. Summary and Discussion.

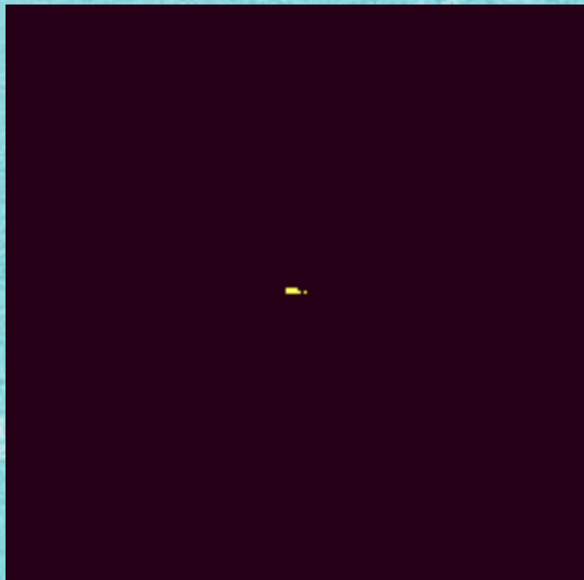

4.1 Correlation between Radio Spectral Index and logR

$$S^{ob} = S_{unb} + S_j^{ob}$$

(Fan et al. 2010)

4.1 Correlation between Radio Spectral Index and logR

$$S^{ob} = S_{unb} + S_j^{ob}$$

$$S^{ob} = S_0^{ob} \cdot \nu^{-\alpha_{total}}$$

$$S_{unb} = S_{unb,0} \cdot \nu^{-\alpha_{unb}}$$

$$S_j^{ob} = S_{j,0}^{ob} \cdot \nu^{-\alpha_j}$$

(Fan et al. 2010)

4.1 Correlation between Radio Spectral Index and logR

$$S_0^{ob} \cdot \nu^{-\alpha_{total}} = S_{unb,0} \cdot \nu^{-\alpha_{unb}} + S_{j,0}^{ob} \cdot \nu^{-\alpha_j}$$

(Fan et al. 2010)

4.1 Correlation between Radio Spectral Index and logR

$$S_0^{ob} \cdot \nu^{-\alpha_{total}} = S_{unb,0} \cdot \nu^{-\alpha_{unb}} + S_{j,0}^{ob} \cdot \nu^{-\alpha_j}$$

differentiating respect to α,

$$\alpha_{total} \cdot S_0^{ob} \cdot \nu^{-\alpha_{total}} = \alpha_{unb} \cdot S_{unb,0} \cdot \nu^{-\alpha_{unb}} + \alpha_j \cdot S_{j,0}^{ob} \cdot \nu^{-\alpha_j}$$

(Fan et al. 2010)

4.1 Correlation between Radio Spectral Index and logR

$$S_0^{ob} \cdot \nu^{-\alpha_{total}} = S_{unb,0} \cdot \nu^{-\alpha_{unb}} + S_{j,0}^{ob} \cdot \nu^{-\alpha_j}$$

differentiating respect to α,

$$\alpha_{total} \cdot S_0^{ob} \cdot \nu^{-\alpha_{total}} = \alpha_{unb} \cdot S_{unb,0} \cdot \nu^{-\alpha_{unb}} + \alpha_j \cdot S_{j,0}^{ob} \cdot \nu^{-\alpha_j}$$

$$\boxed{R = \frac{S_j^{ob}}{S_{unb}}}$$

(Fan et al. 2010)

4.1 Correlation between Radio Spectral Index and logR

$$S_0^{ob} \cdot \nu^{-\alpha_{total}} = S_{unb,0} \cdot \nu^{-\alpha_{unb}} + S_{j,0}^{ob} \cdot \nu^{-\alpha_j}$$

differentiating respect to α,

$$\alpha_{total} \cdot S_0^{ob} \cdot \nu^{-\alpha_{total}} = \alpha_{unb} \cdot S_{unb,0} \cdot \nu^{-\alpha_{unb}} + \alpha_j \cdot S_{j,0}^{ob} \cdot \nu^{-\alpha_j}$$

$$\alpha_{total} = \frac{R}{1+R}\alpha_j + \frac{1}{1+R}\alpha_{unb} \Longleftarrow \boxed{R = \frac{S_j^{ob}}{S_{unb}}}$$

(Fan et al. 2010)

4.1 Correlation between Radio Spectral Index and logR

$$\alpha_t = \frac{R}{1+R}\alpha_{core} + \frac{1}{1+R}\alpha_{Ext}$$

(Fan et al. 2010)

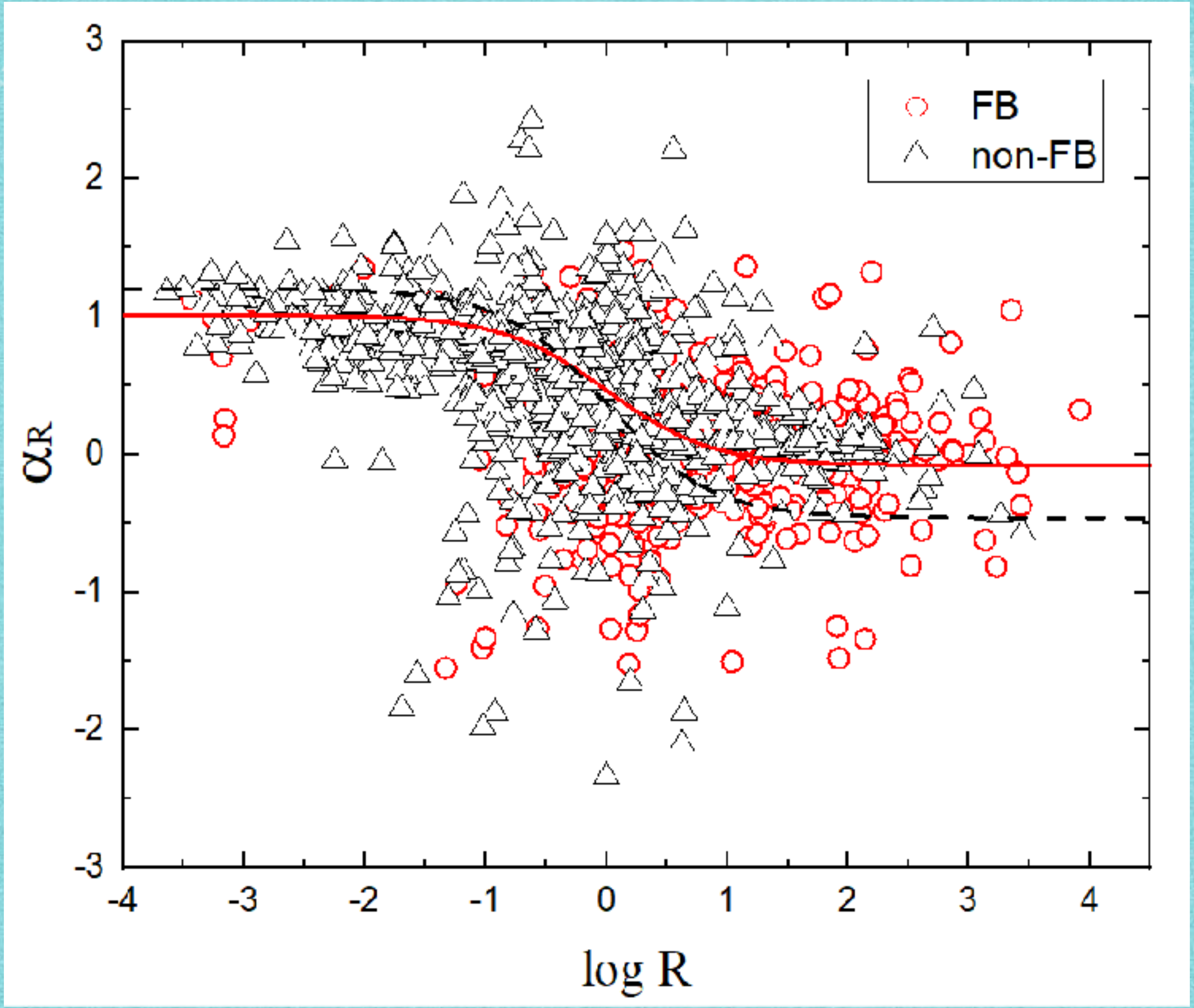

$\boxed{\alpha_{core} = -0.08, \ \alpha_{ext.} = 1.01}$ $\boxed{\alpha_{core} = -0.46, \ \alpha_{ext.} = 1.20}$

(Pei et al. 2018, in prep)

- What about γ-ray emission?

4.2 Correlation between Gamma-Ray Spectral Index and logR

$$\boxed{\alpha_t^\gamma = \frac{R}{1+R}\alpha_{core}^\gamma + \frac{1}{1+R}\alpha_{Ext}^\gamma}$$

(Pei et al. 2016, & 2018, in prep)

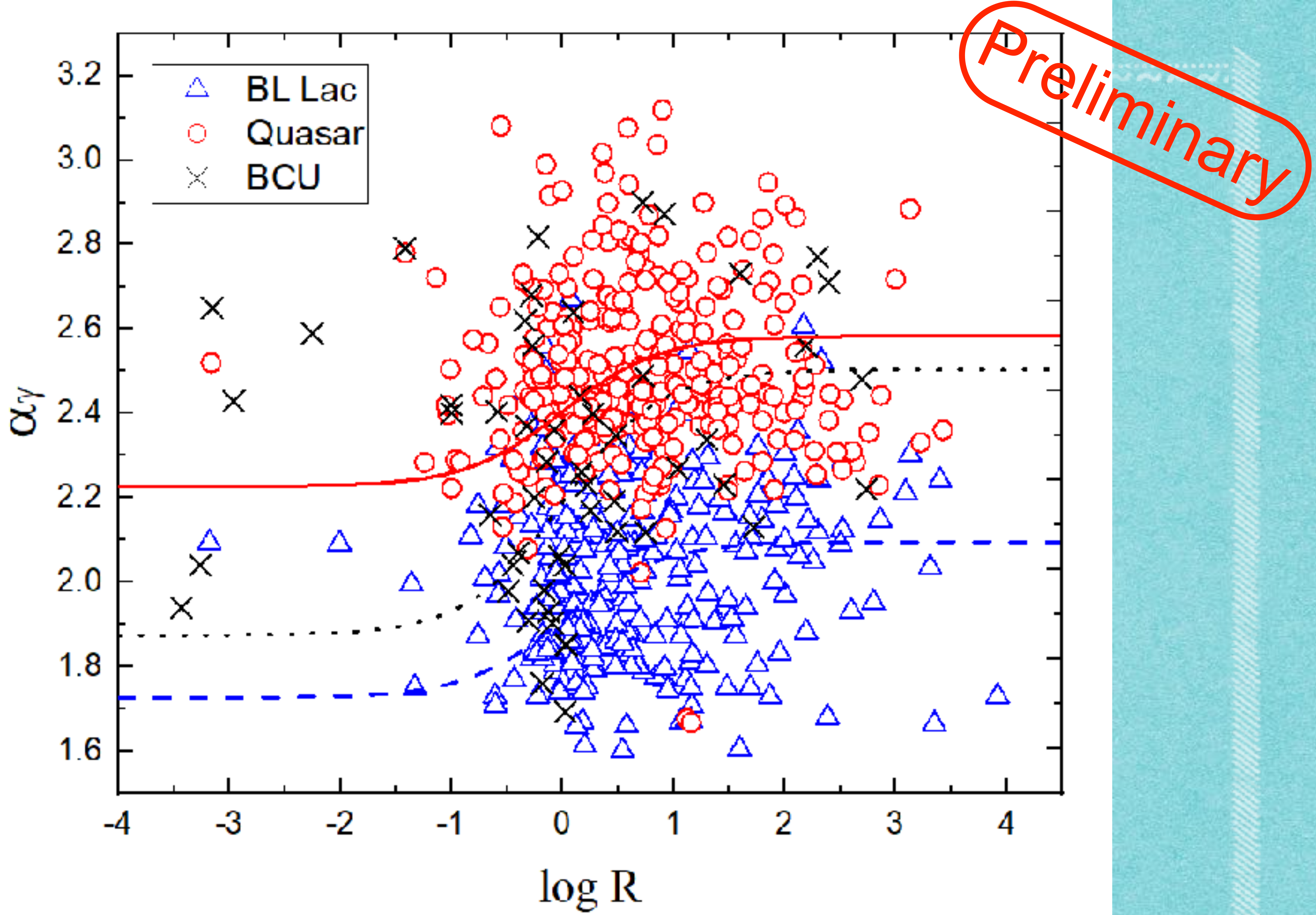

$$\alpha_{core} = 2.09,\ \alpha_{ext.} = 1.72$$

$$\alpha_{core} = 2.58,\ \alpha_{ext.} = 2.22$$

$$\alpha_{core} = 2.50,\ \alpha_{ext.} = 1.87$$

4.2 Correlation between Gamma-Ray Spectral Index and logR

Sample	Statistics Result	Fitting Result for α^{γ}_{core}
BL Lacs	2.04	2.09
FSRQs	2.50	2.58
BCUs	2.30	2.50

γ-ray emissions are mainly from ***the core component***.

(Pei et al. 2016, ApSS, 237, 13; & 2018, in Prep)

Outline

- 1. Introduction to Active Galactic Nuclei and Beaming Effect;
- 2. Fermi Large Area Telescope;
- 3. Core-Dominance Parameter and Data Analysis;
- 4. Correlation between Spectral Index and Core-Dominance Parameter;
- **5. Summary and Discussion.**

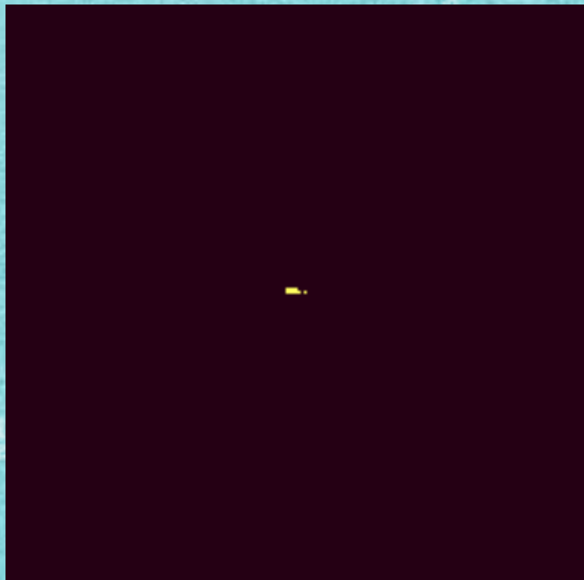

- 1. This is the preliminary results due to adopting the data from FL8Y, we will compile it again respect to 4FGL catalogue after releasing!

- 2. Core dominance parameter (logR) in Fermi blazars (FBs) is quite different from that in non-Fermi blazars (non-FBs). The mean value for FBs is **higher** than non-FBs. So the γ-ray blazars are more radio core-dominated.

- 3. γ-ray emissions are perhaps composed of two components, and the emissions are mainly from the **core (jet)** component.

- 4. Core dominance parameter implies that the Fermi blazars are **beamed!**

Poster!!

The SEDs and Beaming Effect for Fermi Blazars

Junhui Fan, J. H. Yang, Yi Liu, Y. T. Zhang, L. X. Zhang, Y. H. Yuan, J. T. Zhu, Z. Y. Pei, S. L. He

Center for Astrophysics, Guangzhou University, Guangzhou 510006, China

Abstract

In this work, we will report the SED calculations of a sample of 1392 Fermi blazars. Some correlations, including the synchrotron peak frequency vs luminosity correlations, based on the calculations are discussed. Our results show that there are anti correlation between the luminosity (radio, X-ray, gamma- ray, and peak luminosity) and the peak frequency. However, there are positive correlation for the de-beamed luminosity and the peak frequency.

1. SEDs for 1425 Fermi Blazars from 3FGL

Calculating the SEDs for 1425 Fermi blazars from 3FGL using their multiwavelength flux density by fitting

$$\log \nu F_\nu = P_1 (\log \nu - P_2)^2 + P_3$$

SEDs are successfully obtained for 1392 sources. To do correlation analysis (Fan et al. 2016, ApJS, 226, 20).

4. Beaming Effect in Fermi Blazars

Here, we investigate the correlation between the luminosity and the peak frequency for the observed data and the intrinsic data of a sample of Fermi Blazars with available Doppler factors. We found that there is an anti-correlation for the observed data but a positive correlation for the intrinsic (de-beamed value) (Fig. 3). The results suggest that the anti-correlation maybe from a selection effect (Fan et al. 2017, ApJL, 835, 38).

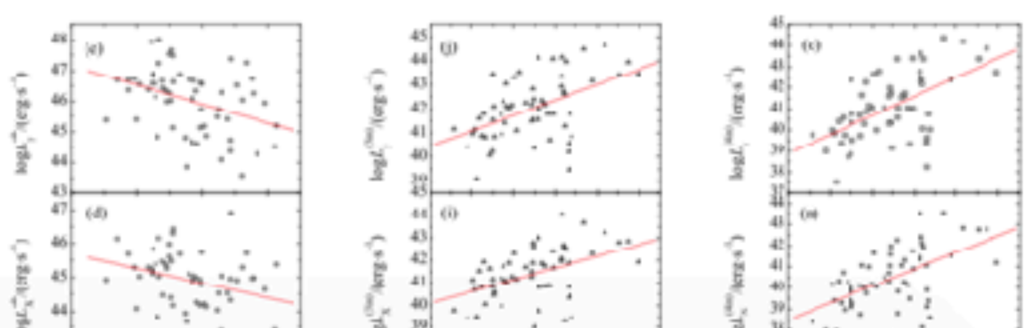

Your comments are welcomed!

- 谢谢 ！
- Grazie!